archives
of thermodynamics
Vol. **31**(2010), No. 1, 45-59
DOI: 10.2478/v10173-010-0003-z

Control-volume-based model of the steam-water injector flow

ROMAN KWIDZIŃSKI*

The Szewalski Institute of Fluid Flow Machinery of the Polish Academy of Science, Fiszera 14, 80-231 Gdańsk, Poland

Abstract The paper presents equations of a mathematical model to calculate flow parameters in characteristic cross-sections in the steam-water injector. In the model, component parts of the injector (steam nozzle, water nozzle, mixing chamber, condensation wave region, diffuser) are treated as a series of connected control volumes. At first, equations for the steam nozzle and water nozzle are written and solved for known flow parameters at the injector inlet. Next, the flow properties in two-phase flow comprising mixing chamber and condensation wave region are determined from mass, momentum and energy balance equations. Then, water compression in diffuser is taken into account to evaluate the flow parameters at the injector outlet. Irreversible losses due to friction, condensation and shock wave formation are taken into account for the flow in the steam nozzle. In two-phase flow domain, thermal and mechanical nonequilibrium between vapour and liquid is modelled. For diffuser, frictional pressure loss is considered. Comparison of the model predictions with experimental data shows good agreement, with an error not exceeding 15% for discharge (outlet) pressure and 1 K for outlet temperature.

Keywords: Balance equations; Supercritical steam-water injector; Irreversible losses; Thermodynamic nonequilibrium; Condensation

Nomenclature

A – cross-section surface area, m^2
c_v – velocity coefficient, dimensionless

*E-mail address: rk@imp.gda.pl

h	–	specific enthalpy, J/kg
$\dot{m}$	–	mass flow rate, kg/s
p	–	pressure, Pa
s	–	specific entropy, J/kg K
T	–	temperature, K
$\bar{T}_{MC}$	–	logarithmic mean temperature difference between steam and water in mixing chamber, K
$\dot{V}$	–	volumetric flow rate, m^3/s
w	–	velocity, m/s
x	–	vapour fraction, dimensionless
z	–	axial coordinate, distance from mixing chamber inlet, m

Greek symbols

α	–	heat transfer coefficient, W/m^2 K
β	–	taper (convergence) angle of the mixing chamber walls, rad
φ	–	void fraction
ρ	–	density, kg/m^3
ζ	–	flow resistance coefficient, dimensionless
ω	–	entrainment ratio, $\dot{m}_{L0}/\dot{m}_{V0}$, dimensionless

Subscripts

CW	–	condensation wave
L	–	liquid (water)
MC	–	mixing chamber
s	–	isentropic flow
sat	–	saturation
t	–	steam nozzle throat
V	–	vapour (steam)
0	–	steam injector inlet
1	–	mixing chamber inlet
2	–	mixing chamber throat
3	–	high-pressure side of condensation shock wave
4	–	steam injector outlet

1 Introduction

In a steam-water injector, thermal energy of motive steam is used to pump and heat the cold water. Recently, new applications of steam injectors in power industry have been studied. One of them is a proposal to use the injectors as feedwater heaters in the thermal power plant [1,2]. The most important advantage of steam injector is its reliability due to lack of moving parts and possibility to work without electric power supply. Steam injector is also a relatively small device. Due to its pumping action, application of the injector as feedwater heater also offers reduction of power used to force the condensate into the boiler.

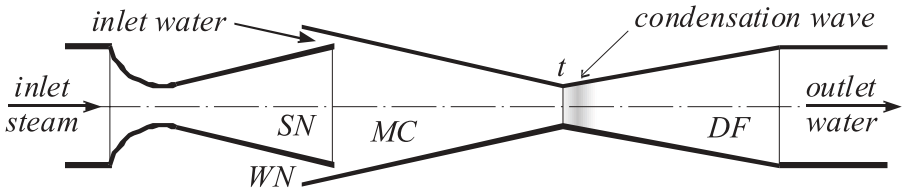

Figure 1. Schematic view of the steam injector: *SN* – steam nozzle, *WN* – water nozzle, *MC* – mixing chamber, *DF* – diffuser, *t* – mixing chamber throat.

Schematic view of the steam-water injector with central steam nozzle is shown in Fig. 1. The injector is driven by steam which is expanded and accelerated in the steam nozzle (SN). Subsequently, the steam enters the mixing chamber (MC), creating there a low static pressure, sufficient for the water to be drawn into the MC through an annular slot surrounding the SN outlet. In the mixing chamber, both phases – having different temperatures and velocities – exchange mass, momentum and energy during condensation of vapour at contact surface with the liquid (water). Resulting two-phase flow is compressed in a pressure wave developing in diffuser (DF) downstream of the throat (t). Inside the wave, the flow velocity decreases substantially and the vapour phase completely condenses. Thus only liquid water is leaving the steam injector at a pressure that in some conditions could exceed the inlet pressure of the motive steam. This is a unique feature of the steam-water injectors brought about by additional contribution of the motive steam thermal energy to the flow momentum in the mixing chamber.

In spite of the steam-water injector simple construction, flow modelling in this device is a challenging task, particularly in the region of two-phase flow present in the mixing chamber and condensation wave. There, a wide range of phenomena should be taken into account, such as the mechanical and thermodynamic non-equilibrium, heat transfer between steam and water, flow-pattern transitions and wave phenomena. Yet, a lot of valuable information may be obtained from a simple model based on integral balances, which are written in control volumes embracing separately each of the injector's distinctive flow regions. The model based on this approach is appropriate for injectors with central steam nozzle working in a wide range of parameters of motive steam, which can be expanded in the steam nozzle to a sub- or supercritical velocity.

2 Model equations

In the proposed model, the flow domain is divided into control volumes comprising the water nozzle, steam nozzle, mixing chamber, condensation wave region and diffuser. The solution is obtained for given flow parameters at the injector inlet (location '0' in Fig. 2). First, the flow equations for steam and water nozzle are solved to determine conditions at the mixing chamber inlet (denoted by '1'). Then, the solution of the mass, momentum and energy balance in the mixing chamber provides data to solve equations in the next control volume, that is in the condensation wave region (between cross-sections '2' and '3'). Finally, Daniel Bernoulli's equation for the liquid-water flow in diffuser is solved to obtain pressure and velocity at the injector outlet ('4'). The equations valid at the interfaces of control volumes considered in the model are given below.

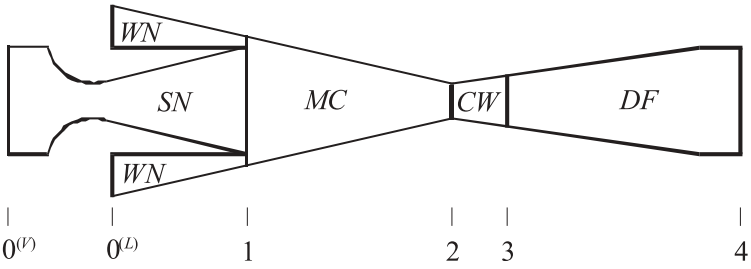

Figure 2. Division of steam injector flow domain into the control volumes comprising: *SN* – steam nozzle, *WN* – water nozzle, *MC* – mixing chamber, *CW* – condensation wave, *DF* – diffuser.

Steam nozzle It is assumed that the flow in the steam nozzle is adiabatic with irreversible losses. The steam properties at the nozzle outlet are determined from the mass and energy balance in the form:

$$A_{V0}\rho_{V0}w_{V0} = A_{V1}\rho_{V1}w_{V1} \quad \text{or} \quad \dot{m}_{V0} = \dot{m}_{V1}, \tag{1}$$

$$h_{V0} + \frac{w_{V0}^2}{2} = h_{V1s} + \frac{w_{V1s}^2}{2} = h_{V1} + \frac{w_{V1}^2}{2}, \tag{2}$$

where subscript s denotes value attained in isentropic expansion (i.e. $s_{V1} = s_{V0}$). In the real flow, irreversible losses reduce the outlet velocity w_{V1}, which is modelled by velocity coefficient c_v defined as

$$c_v = \frac{w_{V1}}{w_{V1s}}. \tag{3}$$

This coefficient takes into account irreversible losses originating not only from friction but also from condensation (when expanding steam crosses the Wilson's line) and shock wave formation near the nozzle outlet (if the pressure in mixing chamber do not match design value). The value of c_v for the injector's steam nozzle was determined from experimental data in [3] and is quoted to be close to 0.9.

With relation (3), double equation (2) can be rewritten to give the steam nozzle outlet enthalpy and velocity,

$$h_{V1} = h_{V1s} + \left(1 - c_v^2\right) \frac{w_{V1s}^2}{2} = c_v^2 h_{V1s} + \left(1 - c_v^2\right) \left(h_{V0} + \frac{w_{V0}^2}{2}\right), \tag{2a}$$

$$w_{V1} = c_v \sqrt{2\left(h_{V0} - h_{V1s}\right)}, \tag{2b}$$

where $h_{V1s} = h(p_{V1},\, s_{V0})$ is the outlet enthalpy in an ideal (reversible) expansion of steam to the required outlet pressure p_{V1}.

The system of balance Eqs. (1) and (2) is closed with state equations for steam. In a typical steam-water injector, the motive steam is superheated at the injector inlet so the required properties

$$\rho_{V0} = \rho\left(p_{V0}, h_{V0}\right), \quad s_{V0} = s\left(p_{V0}, h_{V0}\right) \tag{4a}$$

follow directly from the steam tables. However, the steam may become wet during the expansion. Then, the state of thermodynamic equilibrium is assumed to hold and standard relations are used to calculate enthalpy and density at the steam nozzle outlet in the case of ideal (isentropic) flow:

$$h_{V1s} = x_{1s} h_{V,sat}\left(p_{V1}\right) + \left(1 - x_{1s}\right) h_{L,sat}\left(p_{V1}\right), \tag{4b}$$

$$x_{1s} = \frac{s_{V0} - s_{L,sat}\left(p_{V1}\right)}{s_{V,sat}\left(p_{V1}\right) - s_{L,sat}\left(p_{V1}\right)}, \tag{4c}$$

and for the flow with irreversible losses:

$$\rho_{V1} = \frac{x_1}{\rho_{V,sat}\left(p_{V1}\right)} + \frac{1 - x_1}{\rho_{L,sat}\left(p_{V1}\right)}, \tag{4d}$$

$$x_1 = \frac{h_{V1} - h_{L,sat}\left(p_{V1}\right)}{h_{V,sat}\left(p_{V1}\right) - h_{L,sat}\left(p_{V1}\right)}. \tag{4e}$$

Above, x denotes the vapour fraction and subscript *sat* denotes property calculated at saturation line.

The method given above is valid for steam expanded to both subcritical and supercritical outlet velocity. In the latter case, the divergent-convergent steam nozzle should be used and the nozzle throat diameter is determined by the steam mass flow $\dot{m}_{V0}$. In the throat, the flow velocity w_{Vt} attains a critical value, which could be calculated from the known relation for adiabatic flow of perfect gas

$$w_{Vt} = c_v w_{Vts} = c_v \sqrt{2 \frac{\kappa}{\kappa + 1} \frac{p_{V0}}{\rho_{V0}}}, \tag{5}$$

where κ is the heat capacity ratio. Similarly, the critical pressure at the throat is calculated from:

$$p_{Vt} = p_{V0} \left(\frac{2}{\kappa + 1} \right)^{\frac{\kappa}{\kappa - 1}}. \tag{6}$$

Enthalpy at the nozzle throat is calculated with account of irreversible losses in a way corresponding to Eq. (2a):

$$h_{Vt} = c_v^2 h \left(p_{Vt}, s_{V0} \right) + \left(1 - c_v^2 \right) \left(h_{V0} + \frac{w_{V0}^2}{2} \right). \tag{7}$$

Now, the throat cross section area A_t could be evaluated as

$$A_t = \frac{\dot{m}_{V0}}{\rho \left(p_{Vt}, h_{Vt} \right) w_{Vt}}. \tag{8}$$

It should be noted that in the wet steam region the value of κ is not well defined so the method yields only approximate results.

Water nozzle It is assumed that the pressure at the outlet of water and steam nozzles is the same, $p_{V1} = p_{L1} = p_1$, and that the thermal effect of irreversible losses is negligible. Thus $\rho_{L1} = \rho(p_{V1}, T_{L0})$ and mass balance in the form

$$\dot{m}_{L0} = A_{L1} \rho_{L1} w_{L1} \tag{9}$$

is sufficient to determine the velocity at the nozzle outlet, w_{L1}.

Mixing chamber Two-phase flow in the mixing chamber is modelled taking into account the thermal nonequilibrium and a velocity slip between phases. Thus, the mass, momentum and energy balance for the control

volume between the mixing chamber inlet (cross-section '1', see Fig. 2) and the throat ('2') may be written in the form

$$A_2\rho_2 w_2 = A_{V1}\rho_{V1}w_{V1} + A_{L1}\rho_{L1}w_{L1} \quad \text{or} \quad \dot{m}_2 = \dot{m}_{V1} + \dot{m}_{L1}, \tag{10}$$

$$\dot{m}_2 w_2 + A_2 p_2 + (A_1 - A_2)p_{MC} = \dot{m}_{V1}w_{V1} + \dot{m}_{L1}w_{L1} + A_1 p_1, \tag{11}$$

$$\dot{m}_2\left(h_2 + \frac{w_2^2}{2}\right) = \dot{m}_{V1}\left(h_{V1} + \frac{w_{V1}^2}{2}\right) + \dot{m}_{L1}\left(h_{L1} + \frac{w_{L1}^2}{2}\right), \tag{12}$$

with the assumption that the vapour phase is always saturated and at the throat both phases constitute homogeneous mixture travelling at a common velocity w_2. Thus, the mixture enthalpy h_2 is evaluated from other thermodynamic properties according to relations

$$h_2 = h\left(p_2, \rho_2, T_{L2}\right) = x_2 h_{V,sat}(p_2) + (1 - x_2)h_{L2}(\rho_{L2}, T_{L2}), \tag{13a}$$

$$x_2 = \varphi_2 \frac{\rho_{V,sat}(p_2)}{\rho_2}, \quad \varphi_2 = \frac{\rho_2 - \rho_{L2}(p_2, T_{L2})}{\rho_{V2} - \rho_{L2}(p_2, T_{L2})}. \tag{13b}$$

Contrary to the vapour, the temperature T_{L2} of liquid (water) component of the mixture is usually below the saturation value. This temperature difference (subcooling),

$$\Delta T_{L2} = T_{V,sat}(p_2) - T_{L2}. \tag{14}$$

is an important parameter influencing the flow parameters at the mixing chamber throat. It may be evaluated if the heat transferred per unit time from condensing steam to water is considered. The following equation may be used

$$\dot{m}_c\left[h_{V2,sat}\left(p_2\right) - h_{L2}\left(p_2, T_{L2}\right)\right] = \alpha_{MC} A_{MC} \bar{T}_{MC} \tag{15}$$

with the help of average heat transfer coefficient α_{MC} in the mixing chamber determined by Trela & Butrymowicz [4]. It was assumed in Eq. (15), according to the definition of α_{MC} adopted in [4], that the total heat transfer area A_{MC} equals to the area of the mixing chamber wall and the condensate mass flow rate $\dot{m}_c$ is evaluated from the heat balance in the form

$$\dot{m}_{V1}h_{V1} + \dot{m}_{L1}h_{L1} = \left(\dot{m}_{V1} - \dot{m}_c\right)h_{V2}\left(p_2\right) + \left(\dot{m}_{L1} + \dot{m}_c\right)h_{L2}\left(p_2, T_{L2}\right). \tag{16}$$

To close the model equations for the mixing chamber, an average pressure at the conical wall of the chamber, acting in the flow direction,

$$p_{MC} = \frac{1}{A_2 - A_1}\int\limits_{A_{MC}} p\left(z\right)\cos\frac{\beta}{2}\, dA_{MC}, \tag{17}$$

must also be calculated. Exact p_{MC} value depends on the geometry of the mixing chamber and the pressure $p(z)$ variations along its length. Test calculations have shown that this parameter has minor influence on the model results, so the approximate formula

$$p_{MC} = \frac{p_1 + p_2}{2} \tag{18}$$

is a practical alternative to Eq. (17).

Condensation wave Two-phase flow formed in the mixing chamber is terminated with complete condensation in a pressure wave which is located in the diffuser. If the two-phase flow is supercritical, the wave has properties of a normal shock wave and the flow velocity within it decelerates to a subcritical value. Position of the wave depends on the pressure at injector outlet. For injector working with near-maximum discharge pressure, the condensation wave forms in diffuser immediately downstream of the mixing chamber throat [5]. In this situation the following balance equations are used to determine flow parameters at the high-pressure side of the shock wave region

$$A_3\rho_3 w_3 = A_2\rho_2 w_2 \quad \text{or} \quad \dot{m}_3 = \dot{m}_2, \tag{19}$$

$$\dot{m}_3 w_3 + A_3 p_3 + (A_2 - A_3)p_{SW} = \dot{m}_2 w_2 + A_2 p_2, \tag{20}$$

$$\dot{m}_3 \left(h_3 + \frac{w_3^2}{2} \right) = \dot{m}_2 \left(h_2 + \frac{w_2^2}{2} \right). \tag{21}$$

As vapour completely condenses, only liquid water leaves this region and the enthalpy h_3 is calculated from the state equation in the form

$$h_3 = h\left(p_3, \rho_3\right). \tag{22}$$

In analogy with p_{MC}, a simplified formula

$$p_{SW} = \frac{p_2 + p_3}{2} \tag{23}$$

may be used for evaluation of the flow pressure acting on diffuser wall in the shock wave region.

Location of the cross-section '3' and thus the width of the shock wave region must be known beforehand. Experimental investigation of pressure profile in this region [6] indicates that the value of about 4 cm is a good approximation.

Diffuser Due to deceleration of water in a diffuser, some pressure increase is observed in this part of the injector. So, to calculate the injector outlet pressure p_4, the Daniel Bernoulli equation is used,

$$\frac{p_4}{\rho_4} + \frac{w_4^2}{2} = \frac{p_3}{\rho_3} + (1-\zeta)\,\frac{w_3^2}{2}, \tag{24}$$

with outlet velocity w_4 found from the mass balance,

$$w_4 = \frac{A_3}{A_4} w_3. \tag{25}$$

In the above equations, water incompressibility was assumed, $\rho_3 = \rho_4$. Frictional pressure loss is accounted for in Eq. (24) by the resistance coefficient ζ, which value, in general, is a function of Reynolds number as well as the diffuser length and angle. Empirical correlations or data tables for ζ can be found in handbooks, e.g. in [7]. For the flow in the injector diffuser, the ζ value is typically in the range $0.1 \div 0.2$. The thermal effect of friction is negligible, so outlet temperature T_4 may by considered being equal to T_3.

3 Example calculations and comparison with experiment

The above set of the nonlinear algebraic model equations should be solved successively for the injector component parts or flow regions, beginning with the steam and water nozzle, then proceeding to mixing chamber and condensation wave region, and finishing with the diffuser. In the solution procedure, for given flow parameters at the injector inlet (state '0'), a set of values defining flow conditions at control cross-sections '1', '2' and '3' as well as at the injector outlet '4' is obtained. Solution of the equations for the mixing chamber and the condensation wave region requires employment of iterative numerical method. The known and unknown variables for each solution stage are summarized in Tab. 1.

3.1 Experimental data

The model predictions and accuracy have been tested on the experimental data obtained during tests at the Szewalski Institute of Fluid-Flow Machinery (IFFM) of the Polish Academy of Science on a laboratory-scale supercritical steam-water injector. Details of these experiments can be found in

Table 1. Summary of model variables.

control volume	closure parameters	variables	
		given	sought
steam nozzle (0-1)	c_v	p_{V0}, h_{V0}, w_{V0}, $\dot{m}_{V0}$, p_{V1}, A_{V0}, A_{V1}	h_{V1}, w_{V1}, x_1
water nozzle (0-1)	–	p_{V1}, T_{L0}, $\dot{m}_{L0}$, A_{L0}, A_{L1}	w_{L1}, h_{L1}
mixing chamber (1-2)	ΔT_{L2} or $\bar{\alpha}_{MC}$ and A_{MC}	p_{V1}, h_{V1},h_{L1}, w_{V1}, w_{L1}, x_1, $\dot{m}_{V0}$, $\dot{m}_{L0}$, A_1, A_2	p_2, h_2, w_2, ρ_2
condensation wave (2-3)	L_{SW}	p_2, h_2, w_2, ρ_2, $\dot{m}_2$, A_3	p_3, h_3, w_3
diffuser (3-4)	ζ	p_3, ρ_3, w_3, $\dot{m}_3$, A_4	p_4, T_4, w_4

[8,9]. During the experiments three versions of the injector were investigated, differing in geometry of the mixing chamber throat. In the first version, named SI-A, convergent mixing chamber passed directly into divergent diffuser. When tapered needle was inserted into the mixing chamber throat, the second version was obtained, referred to as SI-B. The third version, the SI-C, was created after a cylindrical passage was inserted into the throat (the needle was not used then). Differences between these three injector versions are illustrated in Fig. 3.

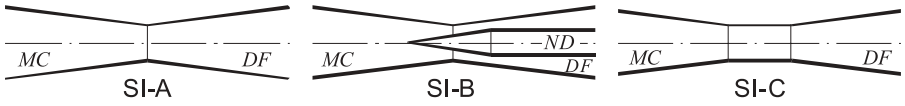

Figure 3. Geometry of the mixing chamber throat in three versions of steam-water injector (SI-A, -B, -C) investigated experimentally at IFFM PASci: *MC* – mixing chamber, *DF* – diffuser, *ND* – tapered needle.

The parameters measured and recorded during the experiments included steam and water inlet temperature, pressure and flow rate as well as distributions of pressure and temperature along the mixing chamber and diffuser. The pressure was also measured at the injector outlet. The construction of the injector allowed for variations of inter-phase exchange conditions in the mixing chamber, to some extent, by adjusting the size of water nozzle gap. The inlet steam flow could also be varied by insertion of a needle into steam nozzle throat. The water was pumped (not sucked) into mixing chamber to widen the range of entrainment ratio $\omega = \dot{m}_{L0}/\dot{m}_{V0}$ variations. The measurements were taken in the following range of the inlet parameters: steam

flow 85÷130 kg/h, absolute steam pressure 3.9 ± 0.2 bar, steam superheating 0÷40 °C, water flow 1÷6 m^3/h, water nozzle gap 0.5÷1.5 mm. The value of the back-pressure at the injector outlet was adjusted by a control valve. This valve was slowly closed until the two-phase flow in the mixing chamber became unstable (i.e. the so-called stalling occurred). Then, the maximum back-pressure was found from the records.

Typical measurements of pressure and temperature distributions along the mixing chamber and diffuser, recorded for selected values of inlet water flow rate, are shown in Fig. 4. The results of maximum back-pressure investigation are illustrated in Fig. 5 where the ratio of this pressure to inlet vapour pressure, p_4/p_{V0}, and corresponding outlet temperature T_4 are depicted as a function of entrainment ratio ω.

Similar experiments, but on a larger scale, were performed at SIET IETI in Italy. Data from these investigations [10, 11] were also used in the model validation.

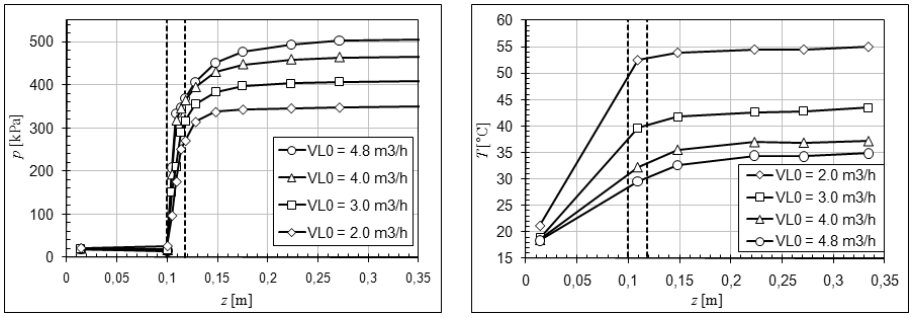

Figure 4. Distributions of pressure p and temperature T at the channel wall measured along the mixing chamber and diffuser of the injector SI-C, recorded for selected values of inlet water flow rate $\dot{V}_{L0}$ at fixed inlet flow parameters ($p_{V0} = 406$ kPa, $\dot{m}_{V0} = 130$ kg/h, $T_{L0} = 18^{\circ}$C). Dashed line indicates the extent of cylindrical throat.

3.2 Calculation results

Model equations were solved for the flow in steam-water injector of geometry and inlet parameters the same as in the experiments described above. The calculation results are shown in Figs. 6÷8. Comparison of typical measured pressure and temperature profiles with calculated values at the model control cross-sections is shown in Fig. 6 for the injectors investigated at IFFM PASci and SIET IETI. It can be noted that on the boundaries of the con-

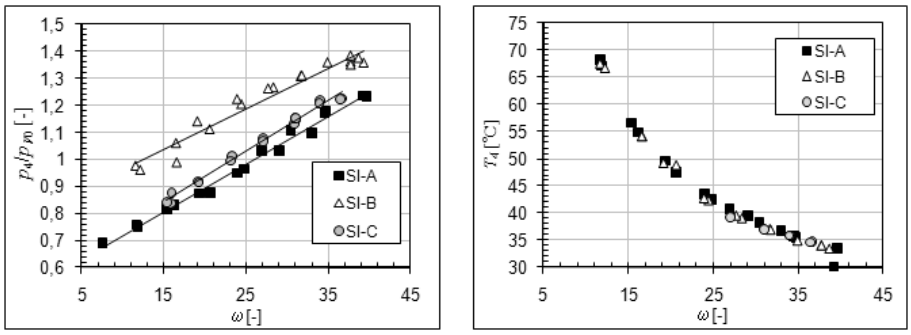

Figure 5. The ratio of inlet-to-outlet pressure p_4/p_{V0} and outlet temperature T_4 versus entrainment ratio ω measured for three versions of IFFM PASci steam injector working with maximum discharge pressure.

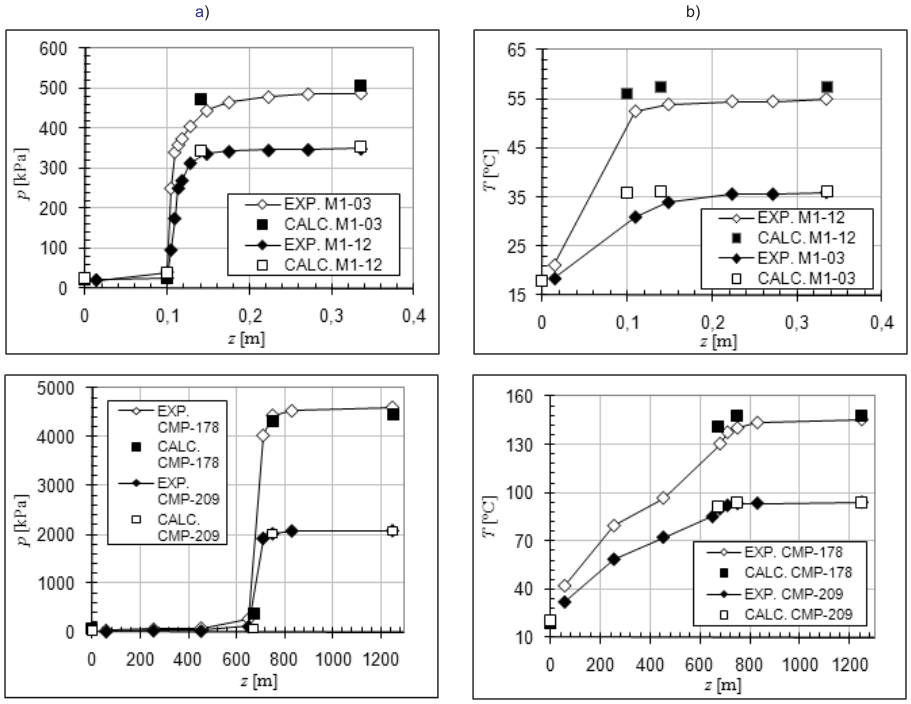

Figure 6. Comparison of typical measured pressure and temperature profiles with calculated values at the model control cross-sections 1÷4: a) IFFM PASci tests, b) SIET Italy tests.

densation wave region (i.e. at cross-sections '2' and '3'), good agreement was achieved for the pressure values but the calculated temperature values are too high. Calculated temperature rise inside the shock wave region is also smaller than observed in experiments. This may indicate that the mixing of freshly-condensed hot water and cooler liquid film flowing close to the channel wall is a relatively slow process that extends beyond downstream boundary of the condensation wave region. Such mixing mechanism is not included in the model and the average temperature calculated differs from the wall temperature measured. Despite that, the calculated outlet temperature is in good agreement with the measured one.

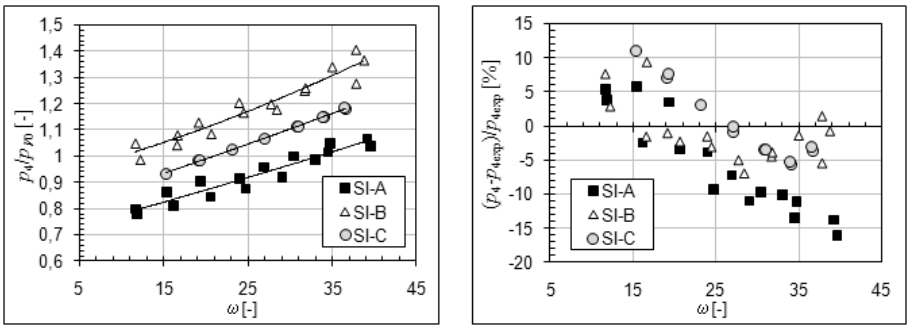

Figure 7. Calculated maximum discharge pressure and the calculation error for the three injector versions with inlet parameters identical to conditions during measurements shown in Fig. 5.

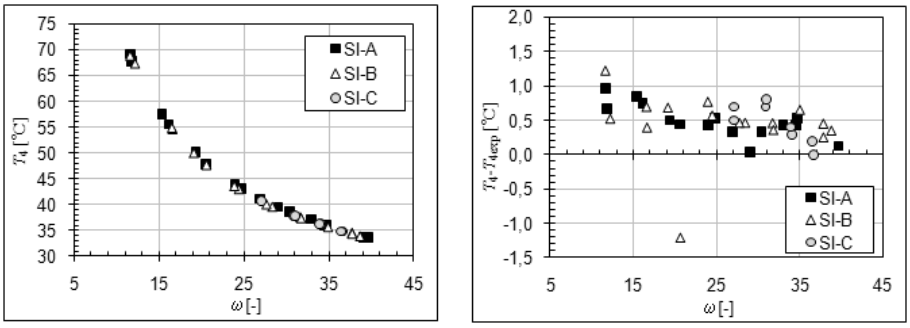

Figure 8. Temperature calculated at the steam injector outlet and the calculation error for flow conditions identical to measurements shown in Fig. 5.

Figure 7 shows calculated values of the maximum outlet (discharge) pressure for the three injector versions investigated experimentally at IFFM

PASci. Similar diagrams for outlet temperature are presented in Fig. 8. These results can be compared to the measurements depicted in Fig. 5. The comparison shows good agreement, with an error not exceeding 15% for discharge pressure and 1 K for the outlet temperature

4 Conclusions

In the paper, a simple mathematical model of the steam-water injector has been presented, which is based on balance equations integrated over control volumes comprising the flow in component parts of the injector. For given parameters at the injector inlet, the model predicts outlet (discharge) pressure, temperature and velocity as well as the flow conditions in control cross-sections placed at mixing chamber inlet and throat as well as at the end of the region comprising condensation wave. It accounts for irreversible losses in the steam nozzle due to friction, condensation and shock wave formation. In two-phase flow in the mixing chamber and the condensation wave, thermal (temperature difference between vapour and liquid) and mechanical (velocity slip) nonequilibrium between phases are taken into account. For diffuser, frictional pressure loss is considered. The model could be applied to performance calculations of injectors with central steam nozzle working at sub- or supercritical flow velocity and with near-maximum discharge pressure.

Example calculations with the model equations confirmed experimental findings concerning dependence of discharge pressure on the mixing chamber throat size. Namely, the reduction of the throat cross-section in the mixing chamber to a value approximately equal to the size of the steam nozzle throat results in a rise of discharge pressure by about 20% (without deterioration of the flow stability).

The model also explains the advantage of cylindrical throat in supercritical steam injector (as in SI-C investigated experimentally at IFFM PASci). In supercritical injectors, the condensation wave has attributes of a shock wave. When the wave is located in a cylindrical channel, which is the case when the injector works with high discharge pressure, there is no pressure loss due to deceleration of supercritical flow in divergent diffuser. In other words, the area $A_2 = A_3$ and the term with p_{SW} in momentum balance (20) vanish. In this case the shock intensity is greater and, as a result, the discharge pressure of SI-C is higher than that of SI-A, what can be seen in Fig. 5 (experiment) and Fig. 7 (calculation).

Received 26 June 2009

References

[1] Narabayashi T., Ohmori S., Mori M., Asanuma Y., Iwaki Ch.: *Development of multi-stage steam injector for feedwater heaters in simplified nuclear power plant*, Japan Society of Mechanical Engineers International Journal, Series B, **49** (2006), No. 2, 368-376. [http://www.jstage.jst.go.jp/article/jsmeb/49/2/368/_pdf]

[2] Trela M., Kwidziński R., Głuch J., Butrymowicz D.: *Analysis of application of feed-water injector heaters to steam power plants*, Polish Maritime Research, Special Issue No. 1 (63) Vol. 16(2009), 62-67.

[3] Trela M., Kwidziński R.: *Influence of the expansion in a steam nozzle on the performance of two-phase ejector*, International Seminar on *Ejector/Jet-pump Technology and Application*, Louvain-la-Neuve, Belgium, Sept. 7-9, 2009, Paper No. 10, CD-ROM.

[4] Trela M., Butrymowicz D.: *Investigation of heat transfer in supersonic steam-water injector*, Proc. 10^{th} Int. Conf. on *Heat Transfer and Renewable Sources of Energy 2004*, Międzyzdroje – Szczecin, Poland, 645-652.

[5] Trela M, Kwidziński R., Buła M.: *Maximum discharge pressure of supercritical two-phase steam injector*, Archives of Thermodynamics, **25** (2004), No. 1, 41-52.

[6] Trela M, Kwidziński R., Butrymowicz D., Jaworek A., Dumaz P.: *Studies of physical phenomena of two-phase flow in steam-water injector*, 11^{th} International Topical Meeting on *Nuclear Reactor Thermal-Hydraulics (NURETH-11)*, Avignon, France, Oct. 2-6, 2005, Paper No. 090, CD-ROM

[7] Idelchik I. E.: *Handbook of Hydraulic Resistance*, (3^{rd} Edition), Begell House, New York 1996.

[8] Kwidziński R., Trela M.: *Investigation of steam injector with variable throat cross-section*, Archives of Thermodynamics, **28** (2007), No. 1, 3-14.

[9] Trela M., Butrymowicz D., Dumaz P.: *Experimental investigations of heat transfer in steam-water injector*, 5^{th} International Conference on *Multiphase Flow (ICMF'04)*, Yokohama, Japan, May 30-June 4, 2004, Paper No. 544, CD-ROM.

[10] Ferri R., Achilli A., Gandolf S.: *DEEPSSI Project: IETI Component Test, Experimental Data Report*, Societa Informazioni Esperienze Termoidrauliche (SIET), Document 00 966 RP 02, 2002.

[11] Ferri R., Achilli A., Gandolf S.: *DEEPSSI Project: IETI Additional Component Test, Experimental Data Report*, Societa Informazioni Esperienze Termoidrauliche (SIET), Document 00 987 RP 02, 2002.